university of groningen

University Medical Center Groningen

University of Groningen

Blooms of Emiliania huxleyi are sinks of atmospheric carbon dioxide

Buitenhuis, Erik T.; van der Wal, Paul; de Baar, Hein J. W.

Published in:
Global Biogeochemical Cycles

DOI:
10.1029/2000gb001292

IMPORTANT NOTE: You are advised to consult the publisher's version (publisher's PDF) if you wish to cite from it. Please check the document version below.

Document Version
Publisher's PDF, also known as Version of record

Publication date:
2001

Link to publication in University of Groningen/UMCG research database

Citation for published version (APA):
Buitenhuis, E. T., van der Wal, P., & de Baar, H. J. W. (2001). Blooms of Emiliania huxleyi are sinks of atmospheric carbon dioxide: A field and mesocosm study derived simulation. *Global Biogeochemical Cycles*, *3*, 577 - 587. https://doi.org/10.1029/2000gb001292

Copyright
Other than for strictly personal use, it is not permitted to download or to forward/distribute the text or part of it without the consent of the author(s) and/or copyright holder(s), unless the work is under an open content license (like Creative Commons).

The publication may also be distributed here under the terms of Article 25fa of the Dutch Copyright Act, indicated by the “Taverne” license. More information can be found on the University of Groningen website: https://www.rug.nl/library/open-access/self-archiving-pure/taverne-amendment.

Take-down policy
If you believe that this document breaches copyright please contact us providing details, and we will remove access to the work immediately and investigate your claim.

Downloaded from the University of Groningen/UMCG research database (Pure): http://www.rug.nl/research/portal. For technical reasons the number of authors shown on this cover page is limited to 10 maximum.

Download date: 05-05-2023

GLOBAL BIOGEOCHEMICAL CYCLES, VOL. 15, NO. 3, PAGES 577-587, SEPTEMBER 2001

Blooms of Emiliania huxleyi are Sinks of atmospheric Carbon Dioxide: A Field and Mesocosm Study derived Simulation

Erik T. Buitenhuis[1], Paul van der Wal, and Hein J. W. de Baar
Netherlands Institute for Sea Research, Texel, Netherlands

Abstract. During field measurements in a bloom of *Emiliania huxleyi* in the North Sea in 1993, an apparently inconsistent combination of observations was measured: (1) fCO_2 was lower in the center of the bloom than in the surrounding nonbloom areas and undersaturated with respect to the atmosphere in both cases, (2) within the bloom, enhanced sedimentation of coccoliths-containing fecal pellets was observed, (3) a large atmospheric sink of 1.3 mol C m^{-2} was derived, and (4) in the same bloom a positive correlation between $CaCO_3$ and fCO_2 was observed, which was interpreted as an increase of fCO_2 during production of $CaCO_3$. In order to resolve the inconsistency between observations (1, 2, 3) and 4 a one-dimensional three-layer model was constructed. A positive correlation between $CaCO_3$ and fCO_2 was obtained when the model was parameterized with data obtained from field and mesocosm studies. The correlation is a feature of the decay phase of a bloom and represents a decrease of fCO_2 with a decrease of $CaCO_3$. Thus it represents the dissolution and sedimentation of $CaCO_3$ rather than its production. Having resolved the ambiguity within the field data by adding the dimension of time in the model, blooms of *E. huxleyi* can be identified as sinks for atmospheric carbon dioxide. This sink is a function of the calcification to photosynthesis (C:P) ratio of the nitrate-using phytoplankton and is maximal when the C:P ratio is 0.42 (that is, *E. huxleyi* constitutes 97% of the nitrate-using phytoplankton). Rather than using the model for making accurate predictions about the magnitude of this sink, a sensitivity analysis was performed to give a range of magnitudes for the range of parameter values that were obtained during previous studies. Furthermore, gaps were identified in the current knowledge of carbon fluxes within blooms of *E. huxleyi*.

1. Introduction

Calcification (precipitation of $CaCO_3$) decreases alkalinity twice as much as dissolved inorganic carbon (DIC). As the chemical speciation of DIC in seawater has been accurately determined [*Millero*, 1995], it follows that the fugacity of CO_2 (fCO_2) increases. However, calcification by *Emiliania huxleyi* is at least loosely coupled to photosynthesis, which decreases DIC and has a smaller effect on alkalinity. Alkalinity increases during uptake of nitrate (NO_3^-) and phosphate (HPO_4^{2-}) and decreases during uptake of ammonia (NH_4^+). The combined effect of calcification (C) and photosynthesis (P), then, results in a decrease of fCO_2 at C:P production ratios lower than 1.7 during use of nitrate (C:P < 1.2 during use of ammonia) and an increase of fCO_2 at higher C:P production ratios. Blooms of *Emiliania huxleyi* have therefore been suggested as potential sources of CO_2 for the atmosphere. A model of the carbon budget of phytoplankton blooms by *Taylor et al.* [1991] calculated a decreased atmospheric sink for calcifying phytoplankton. *Robertson et al.* [1994] concluded that blooms of *E. huxleyi* may constitute smaller sinks than blooms of noncalcifying algae. This conclusion was based on observations in the North Atlantic Ocean, where fCO_2 was 15 μatm higher in samples with $CaCO_3$ > 18 μ*M* than in samples with $CaCO_3$ < 5.5 μ*M*. *Crawford and Purdie* [1997] calculated an actual increase of fCO_2 in blooms of *E. huxleyi*, but this was found under the extreme conditions of 100% mineralization of particulate organic carbon (POC) and 0% dissolution of $CaCO_3$.

Van der Wal et al. [1995] found that sedimentation of carbon is enhanced in a bloom of *E. huxleyi*, owing to the increased weight of fecal pellets that contain coccoliths. This physical effect of enhanced sedimentation complicates the above mentioned chemical effect of calcification on alkalinity and thereby on fCO_2. Sedimentation of particulate carbon itself will not change the air-sea gradient of CO_2. However, if the carbon remains suspended in the surface waters, then it will eventually be mineralized again, and the end result will be no different from the situation before the start of the bloom, while any material that is sedimented below the thermocline will leave the surface waters undersaturated for carbon dioxide.

To illustrate this point, first a model is considered with two boxes: atmosphere and surface water. This model simulates a bloom with first production and then degradation of both POC and calcite ($CaCO_3$). If the C:P production ratio in the model is lower than 1.7, then during the productive stage, CO_2 will decrease and gas exchange will transport CO_2 from the atmosphere to the sea. During the degradation stage, CO_2 will increase and CO_2 will outgas from the sea to the atmosphere. At

[1]Now at Max Planck Institut für Biogeochemie, Postfach 100164, D-07701 Jena, Germany.

Copyright 2001 by the American Geophysical Union

Paper number 2000GB001292.
0886-6236/01/2000GB001292$12.00

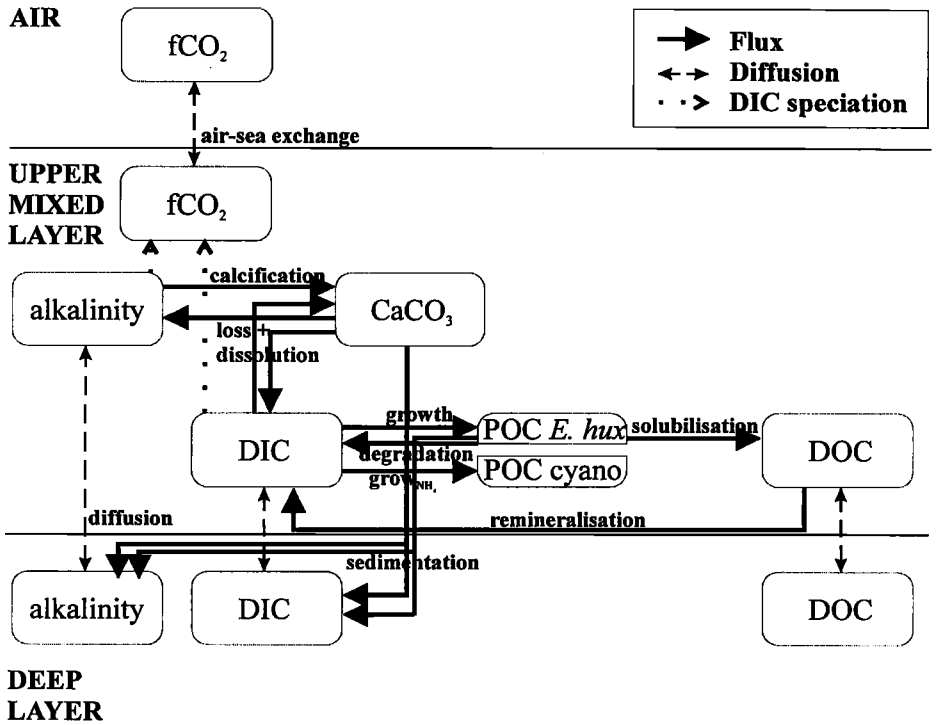

Figure 1. Simplified scheme of the model structure. Pools and fluxes of nitrogen and feedback controls have been omitted. Dotted arrows of DIC speciation indicate that fCO_2 was calculated from DIC and alkalinity (see the "CO_2fromDIC,alkalinity" function in the Notation section for details). Air-sea gas exchange was added to DIC.

the end of the bloom the situation will be the same as at the start, so that the net exchange with the atmosphere will be zero.

This two-box model can be used to illustrate the chemical effect of calcite production. To include the physical effect of calcite in sinking particles, a third box is introduced: the deep sea. The same hypothetical model simulation can now be performed with a bloom in the upper ocean, which is later degraded and some material being transported to the deep layer. Since exchange of dissolved constituents (DIC, alkalinity, etc.) between the upper and the deep layer is slow relative to the production and degradation of the bloom, by the end of the bloom the effect of gas exchange with the atmosphere will be a function of the amount of POC and $CaCO_3$ that is sedimented to the deep layer. The more POC and the less $CaCO_3$ is sedimented, the more CO_2 will be drawn down from the atmosphere. However, if the amount of sedimented POC is stimulated by the amount of heavy $CaCO_3$ in the sedimenting particles then $CaCO_3$ both reduces and increases CO_2 drawdown from the atmosphere. Thus, it has to be determined whether the chemical effect of $CaCO_3$ precipitation is more or less important than the physical effect of $CaCO_3$ enhancing sedimentation. This was done by constructing a three-box model using data from several studies of blooms of *E. huxleyi*.

The model that is presented here includes those processes that were found to occur during both a natural bloom of *E. huxleyi* in the North Sea in 1993 [*van der Wal et al.*, 1995; *Buitenhuis et al.*, 1996; *Wiebinga et al.*, 1999] and a mesocosm study at the field station of the University of Bergen in Raunefjord in 1992 [*van Bleijswijk et al.*, 1994a; *van der Wal et al.*, 1994; *van Bleijswijk and Veldhuis*, 1995]. Parameter values were also taken from these studies.

2. Model Description

The model simulates an algal bloom within a one-dimensional sea with three boxes: an atmosphere with constant fCO_2, a mixed layer with a constant depth of 40 m, and a deep layer of 80 m depth. The model contains 7 carbon pools, 3 nitrogen pools, 2 pools of alkalinity, and a fixed atmospheric fCO_2 (Figure 1). A complete description of the model is given in Tables 1 – 5 and the Notation section. All simulations were run for 60 days with a variable time step to minimize integration errors. Cumulative integration errors were always less than 10^{-12} of the total pools. Most of the parameter values and some of their ranges for the sensitivity analysis were taken from a field study in the North Sea in 1993 [*van der Wal et al.*, 1995; *Buitenhuis et al.*, 1996; *Wiebinga et al.*, 1999] and a mesocosm study in Raunefjorden, Norway, in 1992 [*van Bleijswijk et al.*, 1994a; *van der Wal et al.*, 1994; *van Bleijswijk and Veldhuis*, 1995]. Additional parameter values were taken or derived from *Redfield et al.* [1963], *Alldredge and Gotschalk* [1988], *van Bleijswijk et al.* [1991, 1994b], *Wanninkhof* [1992], *Chipman et al.* [1993], *Roy et al.* [1993], and *Buitenhuis et al.* [1999].

2.1. Model Structure

The model structure is shown in Figure 1 and is described from top to bottom and from left to right. The air has a constant fCO_2 of 360 µatm. In the upper mixed layer, fCO_2 is calculated from alkalinity and DIC with the dissociation constants of *Roy et al.* [1993]. The starting values of alkalinity and DIC were chosen in such a way that the fCO_2 at the start of the model run was 360 µatm at a temperature of 11.6°C and a salinity of 35.2.

Table 1. Differential Equations of the Model

Variable	Equation
$\mu_{E\ hux}$	$\mu_{max,\ E\ hux} \times [NO_3]/([NO_3]+K_{½,\ E\ hux})$
μ_{cyano}	$\mu_{max,\ cyano} \times [NH_4]/([NH_4]+K_{½,\ NH4})$
sedim	SEDIMENTATION
calcif	CALCIFICATION
dissolution	conditional (calcif > $\mu_{max,\ E\ hux}/2$, $diss_{before}$, $diss_{after}$)
$\delta[NO_3]\ \delta t^{-1}$	$-\mu_{E\ hux} \times [POC_{E\ hux}]/$ cn+DIFN/ mld
$\delta[POC_{E\ hux}]\ \delta t^{-1}$	$\mu_{E\ hux} \times [POC_{E\ hux}]$+ (-solubilization -degradation -sedim) × $[POC_{E\ hux}]$
$\delta[POC_{cyano}]\ \delta t^{-1}$	$\mu_{cyano} \times [POC_{cyano}]$
$\delta[NH_4]\ \delta t^{-1}$	degradation × $[POC_{E\ hux}]$/ cn+ remineralization × [DOC]/ cn- $[POC_{cyano}] \times \mu_{cyano}$ / cnh_4
δ[DOC] δt^{-1}	solubilization × $[POC_{E\ hux}]$ -remineralization × [DOC]+ DIFDOC/ mld
δ[DOCdeep] δt^{-1}	-DIFDOC/ dld
$\delta[CaCO_3]\ \delta t^{-1}$	$[POC_{E\ hux}]$ × (calcif- loss × (degradation+ solubilization+ sedim)) × cp- dissolution × $[CaCO_3]$ -sedim × $[CaCO_3]$
δ[DIC] δt^{-1}	$-(\mu_{E\ hux}$-degradation) × $[POC_{E\ hux}]$- $[POC_{E\ hux}]$ × (calcif- loss × (degradation+ solubilization+ sedim)) × cp+ dissolution × $[CaCO_3]$+ remineralization × [DOC]+ DIFDIC/ mld+ AIRSEA- $[POC_{cyano}] \times \mu_{cyano}$
δ[alkalinity] δt^{-1}	-2 × $[POC_{E\ hux}]$ × (calcif- loss × (degradation+ solubilization+ sedim)) × cp+ 2 × dissolution × $[CaCO_3]$+ DIFalk/ mld- $\delta[NO_3]\ \delta t^{-1} \times potAlk_{NO3}$+ $\delta[NH_4]\ \delta t^{-1} \times potAlk_{NH4}$
$\delta[NO_{3deep}]\ \delta t^{-1}$	sedim × $[POC_{E\ hux}]$/ cn × mld/ dld- DIFN/dld
$\delta[DIC_{deep}]\ \delta t^{-1}$	sedim × ($[POC_{E\ hux}]$+ $[CaCO_3]$) × mld/ dld- DIFDIC/dld
$\delta[alkalinity_{deep}]\ \delta t^{-1}$	2 × sedim × $[CaCO_3]$ × mld/ dld -DIFalk/ dld-$\delta[N_{deep}]\ \delta t^{-1} \times potAlk_{NO3}$
$[CO_2]$	CO_2fromDIC,alkalinity
fCO_2	$[CO_2]/K_0 \times 10^6$

The calcification rate (C) is proportional (C:P parameter) to the growth rate (or photosynthesis P) but with a delay. At the start of the model runs, for the length of the delay period, the C:P production ratio is equal to the C:P parameter. After that the C:P production ratio becomes slightly higher than the C:P parameter, until it becomes close to infinite as the NO_3^- concentration approaches 0. The C:P production ratio stays very high for the length of the delay period, after which both calcification and photosynthesis are very small for the remainder of the model run. The delay is introduced because calcification continues after photosynthesis becomes nutrient limited. In cultures, this delay was 2 - 3 days [*Dong et al.*, 1993; *Paasche*, 1998]. In the mesocosm study, calcification rates were still 41% of the average rates 4 days after the peaks of *E. huxleyi* [*van der Wal et al.*, 1994], possibly because nutrients were added daily during this study. Even so, the standing stock of $CaCO_3$ also went through a distinct maximum 2 days after the peak in POC was reached [*van Bleijswijk et al.*, 1994a].

The sedimentation rate is proportional to the sinking rate, calculated with Stokes' law (see the SEDIMENTATION function in the Notation section). This is consistent with the observation that fecal pellets that contain $CaCO_3$ sink rapidly out of the upper mixed layer, whereas fecal pellets without $CaCO_3$ stay suspended in the upper mixed layer for longer periods and are more prone to be degraded there [*van der Wal et al.*, 1995].

Table 2. Output [mol m^{-2}] of the Model

Variable	Equation
Air Sea Flux	ΣAIRSEA × mld × 1000
DOC	[DOC] × mld × 1000
Potential Flux	(ΣAIRSEA +POTFLUX) × mld × 1000
Sedimented $CaCO_3$	Σ(sedim × $[CaCO_3]$) × mld × 1000
Sedimented $POC_{E\ hux}$	Σ(sedim × $[POC_{E\ hux}]$) × mld × 1000

The net growth rate is composed of a gross growth rate and loss factors [*van Bleijswijk et al.*, 1995]. The gross growth rate is a function of nitrate (NO_3^-) according to Michaelis-Menten kinetics [*Michaelis and Menten*, 1913]. The loss rate is composed of sedimentation, solubilization (to dissolved organic matter (DOC)), and degradation (to DIC). The declining phase of the bloom is then brought about by nutrient limitation of the gross growth rate and a loss rate that continues unabated.

The standard model calculates only the C fluxes due to *E. huxleyi*. In reality, the new production of *E. huxleyi* is followed by a secondary growth of cyanobacteria [*Buitenhuis et al.*, 1996]. In one of the runs of the sensitivity analysis, an additional component (POC_{cyano}) was introduced to represent the C flux associated with this secondary growth. In the model, *E. huxleyi* uses only nitrate, while the cyanobacteria use only ammonia. This is a simplification of the observation that new production tends to depend mostly on nitrate, while recycled production uses mostly ammonia. It was chosen as a simple means of representing the complex factors that lead to bloom formation, rather than as a representation of the real situation (which is presented by *Stolte* [1996]). The total primary production was found to be fairly constant throughout the bloom [*van der Wal et al.*, 1995]. Thus, the secondary growth appears to be a recycling

Table 3. Rate Constants in the Model

Process	Description	Value
degradation	$POC_{E\ hux} \rightarrow$ DIC and alkalinity	0.07 d^{-1}
$diss_{before}$	Dissolution $CaCO_3 \rightarrow$ DIC and alkalinity	0 d^{-1}
$diss_{after}$		0.17 d^{-1}
remineralization	DOC → DIC and alkalinity	0.003 d^{-1}
solubilization	$POC_{E\ hux} \rightarrow$ DOC	0.06 d^{-1}
$\mu_{max,\ E\ hux}$	maximum growth rate *E. huxleyi*	0.69 d^{-1}
$\mu_{max,\ cyano}$	maximum growth rate cyanobacteria	0.69 d^{-1}

Table 4. Constants in the Model

Variable	Description	Value
cn	C:N ratio $POC_{E\ hux}$ and DOC	7.4
cnh_4	C:N ratio cyanobacteria	6.625
cp	calcification:photosynthesis ratio	0.433
delay	delay between calcification and photosynthesis	2 d
dld	deep layer depth	80 m
k_{dif}	turbulent diffusion between ml and dl	0.0216 m d^{-1}
k_{av}	CO_2 gas transfer rate	4.229 m d^{-1}
$K_{½,\ E\ hux}$	half-saturation constant *E. huxleyi*	0.1 μM
$K_{½,\ cyano}$	half-saturation constant cyanobacteria	0.1 μM
loss	$CaCO_3$ loss associated with $POC_{E\ hux}$ loss	0.75
mld	mixed layer depth	40 m
$potAlk_{NO3}$	effect of NO_3 and HPO_4^{2-} on alkalinity	1.1396 μeq μM^{-1}
$potAlk_{NH4}$	effect of NH_4^+ and HPO_4^{2-} on alkalinity	0.875 μeq μM^{-1}

pool of carbon and therefore mineralization and sedimentation of this pool are not included.

Diffusive exchange of dissolved constituents between the upper mixed layer and the deep layer is calculated as due to turbulent mixing. Water exchange by variations in the mixed layer depth were not included. For our objective of unraveling general trends, an average wind speed was most suitable. When attempting to simulate a specific bloom, variations in the wind speed can have a large influence (see also 4.1 and *Bakker et al.* [1997]).

2.2. Parameter Values

The processes are described from top to bottom and from left to right as well (Figure 1). The exchange rate between fCO_2 in the air and the upper mixed layer was calculated on the basis of the equation for average wind speeds given by *Wanninkhof* [1992] using the observed average wind speed of 7.2 m s^{-1} [*Buitenhuis et al.*, 1996]. The sum of this exchange is presented as the air-sea flux. At the end of each model run all particulate and organic carbon in the upper mixed layer is mineralized and the flux of CO_2 is calculated to bring the upper mixed layer in equilibrium with the atmosphere. This is added to the air-sea flux during the model run. The results of this flux are presented as the potential flux. Thus, the potential flux is the effect of sedimentation and diffusive exchange between the upper mixed layer and the deep layer, expressed in units of mol CO_2 m^{-2}.

The C:P parameter was calculated as 0.433, on the basis of 20 coccoliths $cell^{-1}$ of 21.7 fmol $CaCO_3$ $coccoliths^{-1}$ per 1 pmol POC $cell^{-1}$ [*van der Wal et al.*, 1994; *Buitenhuis et al.*, 1999].

Dissolution of newly produced coccoliths was undetectable for the first 2 days [*van der Wal et al.*, 1995], but on the other hand the dissolution rate during the end phase of a bloom was 25% per day [*Buitenhuis et al.*, 1996]. About 75% of the coccoliths of a cell were dissolved during loss of a cell [*van Bleijswijk et al.*, 1994a]. In an attempt to combine these observations, dissolution of $CaCO_3$ was composed of two components. During the growth phase of the bloom dissolution is associated by a 75% loss parameter with the three loss factors (sedimentation, solubilization, and degradation). Additionally, during the declining phase of the bloom 17% of the standing stock of $CaCO_3$ dissolves per day, to bring the total dissolution rate to 25% per day.

Nitrate was set at 6 μM at the start of the model run, which was the concentration to the north of the North Sea bloom (M. J. Veldhuis, unpublished manuscript; 1993). Nitrate is taken up by $POC_{E\ hux}$ with a C:N ratio of 7.4 [*Buitenhuis et al.*, 1999]. Ammonia is taken up by POC_{cyano} with a C:N ratio of 6.625 [*Redfield et al.*, 1963]. For both nutrients the $K_{½}$ was 0.1 μM. The effect of uptake and excretion of nitrate, ammonia and phosphate (N:P = 16) on alkalinity was included in the model.

The sedimentation function was based on Stokes' law. In the sensitivity analysis the value of power was -1.32 and -1.08 to give the same total sedimented fluxes as calculated with fixed sedimentation rates of 0.02 and 0.12 d^{-1} [*van der Wal et al.*,1995]. In the standard run, power was set at -1.2. For details, see the description of the SEDIMENTATION function in the Notation section.

A gross growth rate of 0.69 d^{-1} is based on measurements during the growing phase in a mesocosm study [*van Bleijswijk and Veldhuis*, 1995]. A solubilization rate of 0.06 d^{-1} was chosen to give rise to a production of DOC of 0.6 mol m^{-2} [*Wiebinga et al.*, 1999]. A degradation rate of 0.07 d^{-1} was used to give a total loss rate of 0.2 d^{-1} [*van Bleijswijk and Veldhuis* 1995].

DOC is a composite of different molecules with differing biodegradabilities. For practical purposes, DOC can be subdivided into three pools. The most labile fraction is degraded almost as fast as it is produced (viewed on a daily basis). The second fraction can accumulate during algal blooms but is located in the upper mixed layer of these high productivity areas and is thus degraded over timescales at which water transport takes place. The most refractory fraction is degraded only very slowly and can be found as a constant concentration in the deep ocean, and as the background to the more labile pools in the upper ocean [cf. *Wiebinga*, 1999]. The first and last pools have turnover times that fall outside of the scope of this model and the DOC pool in the model represents only the intermediately refractory fraction. A comparison of DOC profiles taken during different stages of the North Sea bloom of *Emiliania huxleyi* has shown that DOC increases up to the peak of the bloom to a concentration of 0.6 mol m^{-2}. The degradation rate was not fast enough to be detectable [*Wiebinga et al.*, 1999]. A low remineralization rate of 0.003 d^{-1} (which gives a half life of 230 days) was used in the standard model and a rate of 0.03 d^{-1} (which gives a half life of 23 days) was used in the sensitivity analysis.

Vertical diffusivities in stratified water vary between ~ 10^{-5} and 10^{-4} m^2 s^{-1} [*Chipman et al.*, 1993]. Since blooms of *E. huxleyi* are normally observed in stable water columns, the lower diffusivity was used in the standard model run, and the higher of the two was used in the sensitivity analysis. Using the equation of *Broecker* [1981]: $K_v = 3.7 \times 10^{-8}\ \delta\rho^{-1}\ \delta z$ (with $\delta\rho\ \delta z^{-1}$ in kg m^{-4}), the diffusivities in the bloom in the North Sea varied between 1×10^{-6} and 6×10^{-6} m^2 s^{-1}. Because the higher diffusivity mentioned above gave virtually the same model output as a diffusivity of 0, these lower values were not used.

In the model, all sedimented material is remineralized instantaneously. Since the model results were not very sensitive to diffusion from the deep layer, this assumption was not explored any further.

Table 5. Initial Concentrations in the Model

Variable	Value
$[alkalinity_{deep}]$	2372 μeq L^{-1}
$[DIC_{deep}]$	2157 μM
$[DOC] = [POC_{cyano}] = [NH_4]$	0 μM
$[NO_{3,\ deep}]$	6 μM
$[POC_{E\ hux}]$	0.1 μM

2.3. BOFS North Atlantic pCO_2 Data

Data of the two cruises with the RRS Charles Darwin (CD60 and CD61) were retrieved from the CD-ROM of the biogeochemical ocean flux study (BOFS, R. K. Lowry et al., 1994; CD-ROM available at http://www.bodc.ac.uk/). The reported pCO_2 was converted to fCO_2 [*Weiss*, 1974].

3. Results

3.1. Model Output

The development of the bloom is characterized by four successive stages.

3.1.1. Stage 1. The growth stage lasts as long as the gross growth rate is higher than the loss rate. At this point, $POC_{E\ hux}$ goes through a maximum, fCO_2 goes through a (local) minimum (Figures 2a and 2d), and nitrate (NO_3^-) is nearly depleted (Figures 2b and 2e). The loss rate is the sum of sedimentation, solubilization ($POC_{E\ hux}$ to DOC), and degradation ($POC_{E\ hux}$ to DIC). Degradation and remineralization (DOC to DIC) release ammonia (Figures 2b and 2e). In the standard model run, which includes only $POC_{E\ hux}$ (Figures 2a-2c), ammonia accumulates (Figure 2b), while in the model run which includes cyanobacteria (Figures 2d-2f), ammonia is used to produce secondary growth of POC_{cyano} (Figure 2e).

3.1.2. Stage 2. At the end of the growth stage, when $POC_{E\ hux}$ growth becomes nutrient limited, $CaCO_3$ production continues for another 2 days, until the dissolution of $CaCO_3$ becomes higher than its production, and $CaCO_3$ goes through a maximum (Figures 2a and 2d). At this point fCO_2 goes through a (local)

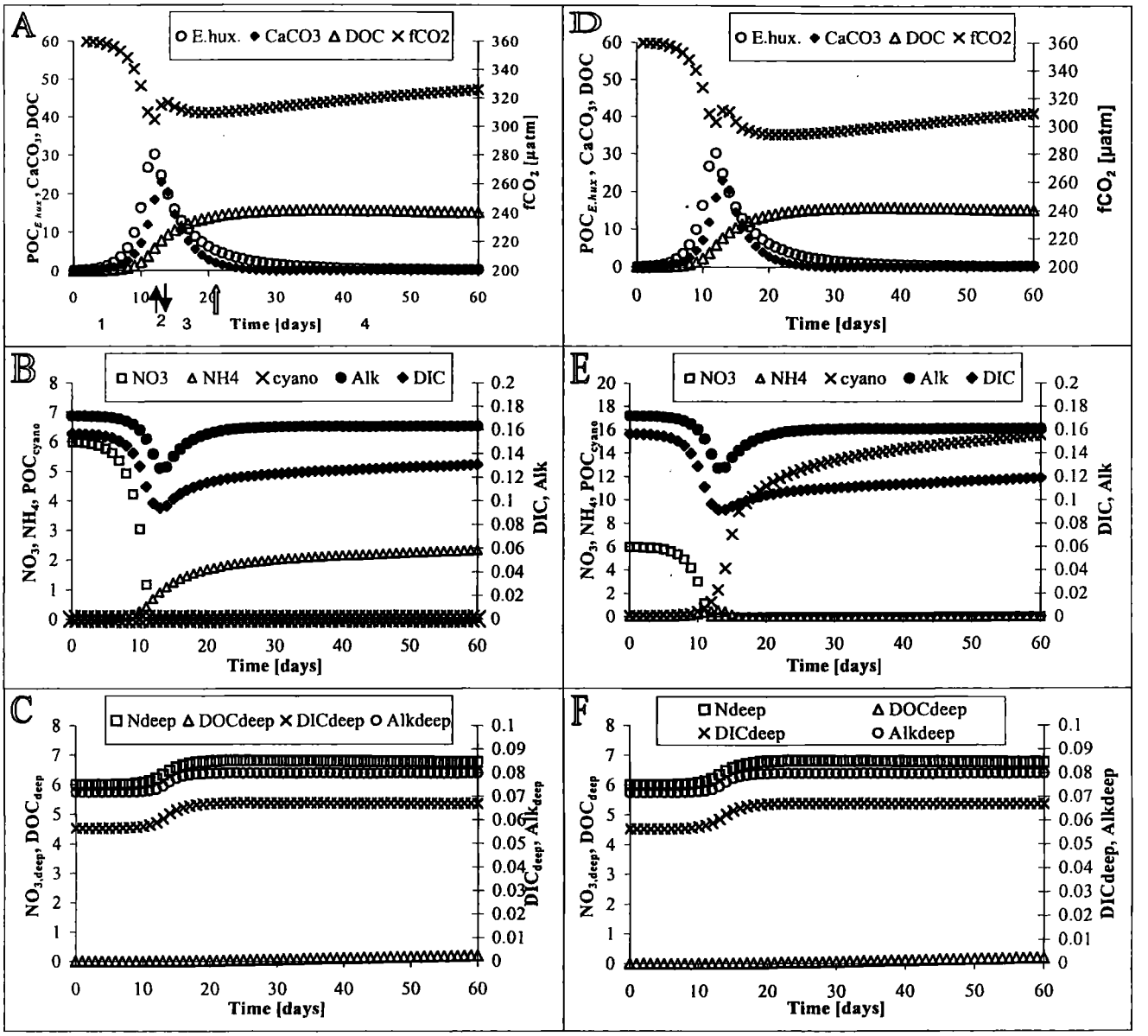

Figure 2. (a-c) Results of the standard run. (d-f) Results including POC_{cyano} using ammonia (NH_4). The successive stages of the bloom marked 1 to 4 are explained in the text. ↑ $POC_{E\ hux}$ maximum, ↓ $CaCO_3$ maximum, ⇑ second fCO_2 minimum. $POC_{E\ hux}$, $CaCO_3$, DOC, NO_3, NH_4, POC_{cyano}, $NO_{3,deep}$, DOC_{deep} in μM, DIC [mM –2], Alk [meq/L – 2.2], DIC_{deep} [mM –2.1], and Alk_{deep} [meq/L –2.3].

maximum. The DOC production rate decreases with the decrease in $POC_{E\ hux}$.

3.1.3. Stages 3 and 4. During the declining phase of the bloom $POC_{E\ hux}$, $CaCO_3$ and DOC are mineralized. Mineralization of $POC_{E\ hux}$ and DOC increases DIC more than alkalinity. In contrast, dissolution of $CaCO_3$ increases alkalinity more than DIC (Figures 2b and 2e).

3.1.4. Stage 3. During the early part of the declining phase, the dominant process is dissolution of $CaCO_3$ and fCO_2 decreases.

3.1.5. Stage 4. During the final stage, air-sea exchange of CO_2 and mineralization of DOC increases the fCO_2. Although depletion of nitrate in the upper mixed layer due to growth (Figures 2b and 2e) and an increase of nitrate in the deep layer by sedimentation (Figures 2c and 2f) create a gradient by which nitrate diffuses upward, this supports only an insignificant amount of $POC_{E\ hux}$ during the final stage (Figures 2a and 2d). The ammonia that is produced by remineralization of DOC gives rise to an increase in POC_{cyano}.

3.2. The fCO_2 as a Function of $CaCO_3$

Figure 3 shows fCO_2 as a function of $CaCO_3$. This shows in a different way from Figure 2 how the fCO_2 decreases when production of $CaCO_3$ is coupled to production of $POC_{E\ hux}$ (stage 1) but increases when production of $CaCO_3$ takes place at the same time as degradation of $POC_{E\ hux}$ (stage 2). During the early part of the declining phase the increase in alkalinity outweighs the increase in DIC and therfore $fCO2$ decreases (stage 3), while in the final stage fCO_2 increases, primarily owing to air-sea gas exchange (stage 4).

3. 3. Sensitivity Analysis

In Table 6 and Figure 4 a sensitivity analysis is given of the model parameters. Two air-sea CO_2 exchange values are given: a short-term flux that occurs during the bloom and a long-term potential flux that is the ultimate effect of the net transport into the deep layer. The short-term flux is the cumulative flux of air-sea exchange during the model run and thus takes into consideration all processes that sequester carbon and is dependent on the time that the model is run. The potential flux is the flux after mineralization of all the particulate and organic carbon in the upper mixed layer and equilibration of the upper mixed layer with the atmosphere. In other words, the potential flux excludes the effect of increased sequestration of carbon (predominantly in DOC and POC_{cyano}) that is degraded in the course of the year and calculates the effective impact of the net transport of DIC, alkalinity and DOC by sedimentation and diffusion to the deep layer (see the POTFLUX function in the Notation section for details).

In the parameters that affect $POC_{E\ hux}$, a clear feedback can be seen between degradation, solubilization and sedimentation (the latter is controlled by the parameter power, see the SEDIMENTATION function in the Notation section). If one of these three rates is increased, this decreases the amount of $POC_{E\ hux}$ that will be passed to the other two processes. In Table 6 it can be seen that if the rates of degradation or sedimentation are increased, the amount of DOC formed is decreased. Likewise, if the rates of degradation or solubilization are increased, the amount of $POC_{E\ hux}$ that is sedimented is decreased. The effect on the amount of $POC_{E\ hux}$ that is degraded is not shown.

The parameters that affect DOC have an opposite effect on the potential flux and the air-sea flux because DOC temporarily sequesters carbon in the upper mixed layer. This DOC will be degraded after the end of the bloom, while the fraction of DOC that is transported to the deep layer by turbulent diffusion is rather limited (Figure 2c).

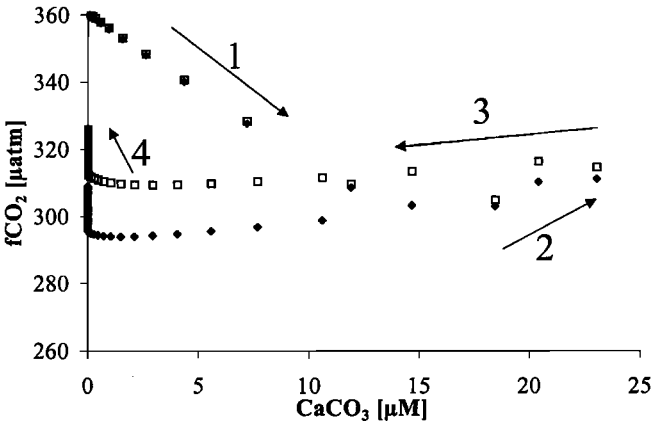

Figure 3. The fugacity of CO_2 (fCO_2) as a function of the $CaCO_3$ standing stock. Arrows indicate the direction of time. The successive stages of the bloom, marked 1-4 are the same as in Figure 2. Squares indicate $POC_{cyano} = 0\ \mu M$ as in Figures 2a-2c; Diamonds indicate $POC_{cyano,\ start} = 0.1\ \mu M$ as in Figures 2d-2f.

The effect of the changes in $CaCO_3$ cycling on the potential flux and the air-sea flux is less straightforward. On the one hand, the chemical effect of production of $CaCO_3$ increases fCO_2 and thus decreases the air to sea exchange of CO_2. On the other hand, the physical effect of inclusion of $CaCO_3$ in fecal pellets increases the sedimentation rate and thus increases the air to sea exchange of CO_2. The relative importance of these two effects was tested by varying the C:P parameter in the model to simulate a varying proportion of *E. huxleyi* in the nitrate-using phytoplankton or a different C:P production ratio by *E. huxleyi*. Variation of the C:P parameter gives rise to a weak optimum for the air-sea exchange and a sharper optimum for the potential flux (Figure 4). The amount of $CaCO_3$ that is sedimented increases quadratically with the C:P parameter, since there is an increase in both the amount of $CaCO_3$ and the fraction of $CaCO_3$ that is sedimented due to the higher density of the sedimented material. The amount of POC that is sedimented increases asymptotically, since the fraction of POC that is sedimented increases to the same extent as $CaCO_3$, but the total amount of POC that is produced from a fixed amount of nitrate stays the same. Thus, the amount of atmospheric CO_2 that is drawn down into the sea goes through a maximum. For the short-term flux the maximum lies at a contribution of 23% *E. huxleyi* of the total POC (C:P = 0.1). For the potential flux the maximum lies at a contribution of 97% of the total POC (C:P = 0.42). The difference between these two is primarily caused by the contribution of DOC to the short-term flux: half of the POC that is not sedimented is converted into DOC, and DOC production increases the air-sea flux but does not affect the potential flux.

3.4. Model Validation

The model is based on the results of a field expedition in the North Sea in 1993 and a mesocosm study near Bergen, Norway, in 1992. In an attempt to verify the validity of the model results with independent data, the model output was compared to data from two field expeditions in the North Atlantic in 1991 that

Table 6. Sensitivity Analysis[a].

Parameter[b]	Value	Air-Sea Flux	Potential Flux	$CaCO_3$ Sedimented	$POC_{E\,hux}$ Sedimented	DOC
Standard run[b]		0.42	0.29	0.37	0.51	0.61
Degradation (0.06)	0.03	0. 47	0. 33	0.38	0.55	0.76
$POC_{E\,hux} \rightarrow$ DIC	0.12	0.34	0.22	0.35	0.43	0.43
Delay (2)	0	0.45	0.17	0.08	0.22	0.74
	3	0.38	0.26	0.57	0.61	0.56
Diffusion (0.0216)	0	0.41	0.30	0.37	0.50	0.60
	0.216	0.43	0.20	0.37	0.52	0.67
Dissolution (0/0.17)	0/0	0.34	0.18	0.84	0.70	0.51
$CaCO_3 \rightarrow$ DIC	0.17/0.17	0.44	0.26	0.19	0.36	0.67
Loss (0.75)	0.44	0.40	0.30	0.48	0.58	0.57
$POC_{cyano,\,start}$ (0)	0.1	0.56	0.29	0.37	0.51	0.61
NO_3 (6 μM)	10 μM	0.65	0.48	0.62	0.85	1.01
Power (-1.2)	-1.08	0.42	0.54	0.51	0.82	0.46
	-1.32	0.42	0.10	0.17	0.21	0.74
Remineralization (0.003) DOC → DIC	0.03	0.34	0.28	0.37	0.51	0.19
Solubilization (0.07)	0.03	0.37	0.34	0.38	0.56	0.36
$POC_{E\,hux} \rightarrow$ DOC	0.14	0.45	0.22	0.34	0.42	0.83

[a] Air Sea Flux, cumulative air-sea gas exchange during the model run; Potential Flux, potential flux to the deep layer; $CaCO_3$ Sedimented and POC Sedimented, cumulative amounts of $CaCO_3$ and POC sedimented to the deep layer; DOC, amount of DOC in the upper mixed layer at the end of the model run. Output in $mol \cdot m^{-2}$.

[b] Values for standard run in parentheses. For dissolution, the two values designate the rates before and after the peak of $POC_{E\,hux}$.

were collected by J. Robertson (CD-ROM available at http://www.bodc.ac.uk/).

In 1991, two cruises with the RRS *Charles Darwin* took samples along the 20°W meridian. During the first cruise, in June, a bloom of *E. huxleyi* occurred south of Iceland. The results of this cruise are described by *Robertson et al.* [1994]. The 0.5° averages show that fCO_2 was 10 μatm. higher between 61° and 63°N, where the bloom of *E. huxleyi* was densest, than between 58° and 60°N (Figure 5a). The data between 61° and 63°N were collected on June 20, which was in the week when the bloom was at its maximum extent [*Robertson et al.*, 1994]. The data of the second cruise were collected 1 month later. At this time the fCO_2 was 9 μatm lower in the region where the bloom had been (61° - 63°N compared to 58° - 60°N, Figure 5a).

For comparison the model output of fCO_2 are shown for the standard model and the model without calcification (C:P = 0). The fCO_2 is 16 μatm higher in the calcifying bloom during the week after the $CaCO_3$ peak (Figure 5b), when blooms are most visible on satellite images owing to shedding of coccoliths by *E. huxleyi*. This is similar to the 15 μatm difference between samples taken at high $CaCO_3$ concentrations compared to low $CaCO_3$ concentrations [*Robertson et al.*, 1994] and higher than the 10 μatm difference in the BOFS data of June 1991. Thirty days after the $CaCO_3$ peak fCO_2 is 0.4 μatm lower in the calcifying bloom. Again this is higher than the -9 μatm difference in the BOFS data of July 1991. For the 1993 bloom in the North Sea, fCO_2 inside the bloom was 21 μatm lower than outside the bloom [*Buitenhuis et al.*, 1996], which is based on samples taken in the course of the declining phase of the bloom.

4. Discussion

4.1. Comparison of the Model Output to the Mesocosm and North Sea Blooms

Although the gross $CaCO_3$ production rate of 0.433 is lower than that found for some other strains, it is consistent with the results for strain CH24 [*Buitenhuis et al.*, 1999], which was isolated from the North Sea in 1990 [*van Bleijswijk et al.*, 1991]. The model outputs are consistent with measurement in the mesocosms of a peak of $CaCO_3$ that is ~ ¾ of the POC peak [*van Bleijswijk et al.*, 1994a] and in the North Sea of an average $CaCO_3$:POC sedimentation ratio of 0.7 [*van der Wal et al.*, 1995].

Comparing the model results to the carbon fluxes that were estimated directly from measurements in the North Sea bloom (1.3 mol C m^{-2} for air-to-sea CO_2-exchange and 2.4 mol C m^{-2} of sedimentation [*Buitenhuis et al.* 1996]), it can be seen that both the air-sea flux and the sedimented flux in the model are about 3 times lower. First of all it can be seen from the sensitivity analysis (Table 6 and Figure 4) that the ranges for the parameter

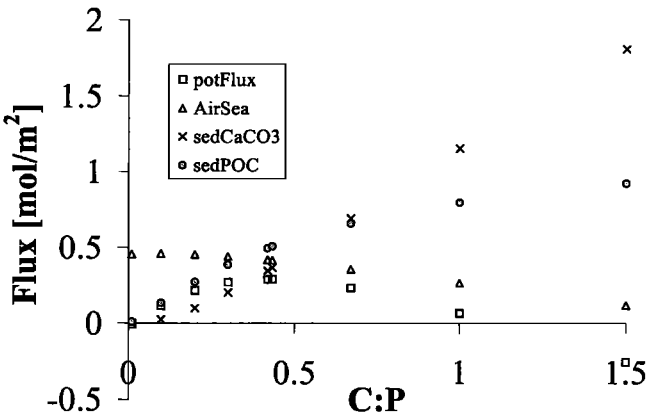

Figure 4. Fluxes in the modeled bloom as a function of the C:P ratio of the nitrate-using phytoplankton ($POC_{E\ hux}$ box). Ammonia is not used (POC_{cyano} = 0 μM). PotFlux is the flux of CO_2 from the atmosphere owing to transport of DIC, alkalinity, DOC, and NO_3^- to the deep layer. AirSea is the flux of CO_2 from the atmosphere during the model run (60 days). $SedCaCO_3$ and sedPOC are the amounts of $CaCO_3$ and $POC_{E\ hux}$ that are sedimented to the deep layer during the model run. Please note that the C:P parameter on the x axis is not the C:P producion ratio, as is explained in section 2.1.

values give a range of model outputs. More importantly, however, there are at least three elements of bias in the model to explain this about threefold difference.

1. The contribution of other organisms to the carbon sink has been purposely ignored in the standard run in order to extract the contribution of *E. huxleyi* alone to the fluxes. The inclusion of a box for the cyanobacteria gives a first approximation of the effect of secondary growth on ammonia, but via microzooplankton, some of this carbon will also be grazed by mesozooplankton or otherwise be transported out of the upper mixed layer [*Koshikawa et al.*, 1999].

2. For the same reason the effects of seasonal warming on fCO_2 and of the wind speed on the surface mixed layer depth have been ignored. The finding that there was a very small correlation between $CaCO_3$ standing stock and water temperature in the 1993 North Sea bloom [*Buitenhuis et al.*, 1996] in the presence of salinity stratification [*Veldhuis*, 1993] suggests that the correlation of water reflectance and water temperature as found by *Ackleson et al.* [1988] may be primarily due to a correlation between high stratification and *E. huxleyi* abundance and not to coccolith reflectance causing warming of the upper mixed layer. The influence of (the variability of) the wind speed on the magnitude of the carbon sink during a bloom depends on the relative importance of three processes with opposing effects: a shallow upper mixed layer during low wind speeds increases light availability for photosynthesis, while high wind speeds increase air-sea gas exchange, and increasing wind speeds deepen the wind mixed layer and thereby entrain nutrient-rich deep waters (E. Hannon et al., manuscript in preparation].

3. The C:N ratio of the dissolved organic matter (DOM) is usually found to be higher than the 7.4 of the DOM or the 6.625 of the cyanobacteria (POM_{cyano}) that is used in the model. This effect was observed as an increase of the particulate POC:PON ratio during the mesocosm bloom [*van Bleijswijk et al.*, 1994a]. By contrast, the C:N ratio of heterotrophic bacteria (which are not included in the model) start to increase only when the substrate C:N ratio is very high and growth rates are low [*Goldman and Dennett*, 2000]. Unfortunately, not enough data are available to include changes in the POC:PON ratio in the model.

Another effect of including POC_{cyano} in the model is to further uncouple the dissolution of $CaCO_3$ from the mineralization of POC. The other mechanism that uncouples these processes is the delay between the peaks of $CaCO_3$ and $POC_{E\ hux}$. This uncoupling gives rise to a decrease in fCO_2 during dissolution of $CaCO_3$ (stage 3 in Figure 3). By including POC_{cyano} the slope of this part of the plot increases from 0.4 to 0.9 $\mu atm\ fCO_2$ ($\mu M\ CaCO_3$)$^{-1}$. The slope that was found during the North Sea bloom was 3.5 $\mu atm\ \mu M^{-1}$, indicating that $CaCO_3$ dissolution, POC remineralization, and secondary growth were even further uncoupled, as indicated by the inverse trends between $CaCO_3$ and POC in this bloom [*Buitenhuis et al.*, 1996].

4.2. Influence of $CaCO_3$ on Air-Sea Exchange of CO_2

Robertson et al. [1994] found an average increase in pCO_2 (a reduction of the sea-to-air gradient) of 15 µatm in a bloom of *E. huxleyi*. This was shown by comparing samples in which $CaCO_3$

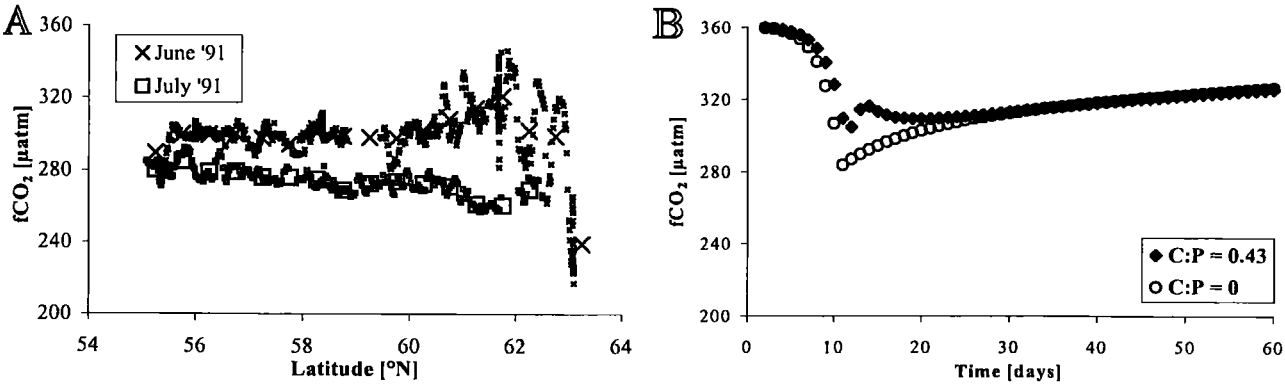

Figure 5. (a) fCO_2 along the 20°W meridian. Crosses indicate the transect sampled from June 16 – 21, 1991, during a bloom of *Emiliania huxleyi*. Transect was sampled from south to north. Squares indicate the transect sampled from July 24 – 26, 1991. Transect was sampled from north to south. (b) Model output of fCO_2 for calcifying (solid diamonds) and noncalcifying (open diamonds) nitrate using algae.

was greater than 18 μM with samples in which $CaCO_3$ was smaller than 5.5 μM. *Buitenhuis et al.* [1996] found an increase in fCO_2 of 3.5 µatm (μM $CaCO_3$)$^{-1}$. *Van der Wal et al.* [1995] found an enhanced sedimentation of both POC and $CaCO_3$ in the latter of these blooms due to the increased density of fecal pellets, loaded with coccoliths, with an inferred increased sinking rate of the fecal pellets. *Buitenhuis et al.* [1996] noted the inconsistency between this increase in fCO_2 and an enhanced sedimentation; and also calculated a carbon sink of 1.3 mol C m^{-2} for this bloom. With the described model these data can be reinterpreted into a consistent explanation. This was possible because the model adds a direction of time to the observations that were collected at different locations in the field studies. The results of the model indicate that the correlation between $CaCO_3$ and fCO_2 (stage 3 in Figure 3) does not represent an increase in fCO_2 as $CaCO_3$ is produced, but a decrease in fCO_2 as $CaCO_3$ is dissolved. This is consistent with the fact that both field studies were conducted during the end phase of the blooms, that is, when they were visible on satellite images due to light scattering of coccoliths [*Robertson et al.*, 1994; *Buitenhuis et al.*, 1996].

Thus, it cannot be concluded from the field data that there is a negative correlation between the amount of $CaCO_3$ that is produced and the air to sea flux of CO_2. Therefore, we have addressed this question anew with the model, by performing a sensitivity analysis of the short-term and long-term air-sea CO_2 fluxes as a function of the C:P parameter (Figure 4). The most significant feature of this correlation is that the air-sea flux is highest at a C:P parameter value greater than 0; in other words, calcification stimulates the air-sea flux up to a certain point, after which it decreases again. The magnitude of the optimum C:P parameter value is subject to our choice of parameters (such as the change in porosity of the fecal pellets by inclusion of $CaCO_3$, which was estimated by an indirect method, see SEDIMENTATION function in the Notation section). However, with recent improvements of the sensitivity in chemical analytical methods, it should now be possible to derive the correlation between the POC and $CaCO_3$ contents in individual fecal pellets (POC: [*Ulrich-Rich et al.*, 1998], $CaCO_3$: within the detection range of graphite furnace AAS) and their densities [*Urban et al.*, 1993] and sinking rates [*Harris*, 1994]. Together with the degradation rate [*Ploug et al.*, 1999] this would give the correlation between the $CaCO_3$:POC ratio in the water column and sedimentation rate in a more direct way.

The density excess of diatom frustules, like that of coccoliths, is much higher than that of organic material. Therefore it might be expected that the same mechanism that was found in a bloom of *E. huxleyi* [*van der Wal et al.*, 1995] would function in blooms of diatoms. However, the results of *Urban et al.* [1993] indicate that this may not be the case, owing to a lower packing index when the dominant food source was diatoms. The density of fecal pellets changed with the diet of the zooplankton, increasing in the order of diatoms, nanoflagellates, and a mixed population including coccolithophores.

4.3. Implication for Paleoreconstruction and Effect of Enhanced Sedimentation on Geological Timescales

Our results indicate that even at a modest nitrate concentration of 6 μM at the start of the bloom approximately half of the biomass is produced at an fCO_2 that is more than 32 µatm lower than at the start of the bloom. This implies that the paleoreconstruction of *Jasper et al.* [1994] may underestimate the oversaturation of upwelling water because their reconstruction of the fCO_2 of upwelled equatorial Pacific waters over the past 225,000 years was based on the $^{13}C/^{12}C$ ratio of alkenones in the sediment that were produced by prymnesiophyte algae (of which *E. huxleyi* is a member). Thus, most of the signal would be produced during periods when algal growth is high and fCO_2 is relatively low. Moreover, this underestimation could have been larger if production during glacial periods would have been higher, so that the glacial to interglacial difference in oversaturation would have been even larger than the presented 50 µatm [*Jasper et al.*, 1994].

When the effect of $CaCO_3$ to stimulate the cosedimentation of POC is extrapolated to geological timescales, the control of the alkalinity budget of the ocean on the cycling of $CaCO_3$ becomes important. The cycling of $CaCO_3$ is not controlled by production. Rather, export of Ca/alkalinity from the upper ocean exceeds import, mostly by rivers, and the excess dissolves in the deep sea. The balance between these processes is maintained by the depth of the saturation horizon of calcite [*Milliman et al.*, 1999]. Since atmospheric CO_2 is not controlled by $CaCO_3$ production in the surface ocean, we suggest that the effect of $CaCO_3$ to stimulate sedimentation of POC may enhance drawdown of CO_2 from the atmosphere even more clearly on long timescales than the presented model results for a seasonal bloom suggest.

5. Summary

Integrating an extensive data set on the cycling of carbon within blooms of *Emiliania huxleyi* into a model, it was shown how a positive correlation of fCO_2 and $CaCO_3$ within blooms can be consistent with an enhanced carbon sink for coccolithophorid blooms. It was found that the air to sea CO_2 flux as a function of the C:P parameter shows an optimum C:P parameter value. While the exact value of the optimum C:P parameter value is influenced by many assumptions in the model, the basic form of this function is due to the three following assumptions: (1) There is a positive correlation between the $CaCO_3$:POC standing stock ratio in the medium and in the fecal pellets. In the model this correlation is 1:1 as found by *Harris* [1994], (2) There is a positive correlation between $CaCO_3$ content of fecal pellets and sinking rate. This is predicted by Stokes' law, (3) There is a positive correlation between sinking rate and sedimentation rate. The model by *Taylor et al.* [1991] reached the opposite conclusion (in their model the atmospheric sink for CO_2 is reduced when phytoplankton produce coccoliths) by not varying the sinking speed of particles as a function of their density. This shows that the dependence of sedimentation on the density of the particles is of critical importance to the conclusions that we draw from the presented model.

Additionally, a shortage of data was identified in the following areas: (1) The rates of production and degradation of DOC, (2) The degradation of POC to DIC, (3) The role of cyanobacteria in using regenerated ammonia and maintaining low fCO_2 pressures during the collapse of the blooms of *E. huxleyi*, and the importance of the coupling between the microbial loop and the classical food chain by microzooplankton and mesozooplankton grazing, (4) The importance of changes in the C:N ratio from new production to DOC and bacterial production to increase the carbon sink per unit of nutrient, and (5) The relationship between the $CaCO_3$ content of fecal pellets and the sedimentation rate. More generally speaking, the processes of production are much better documented than the processes of decline. Rather than claiming to have provided any definitive carbon budget, we hope to have provided some new insights, as a guide towards obtaining a more accurate budget in the future.

Notation: Functions in the Model

AIRSEA = $k_{av} \times (CO_{2,air} - [CO_2])$

CALCIFICATION = $\mu_{E\,hux}$(time – delay).

If time < delay Then CALCIFICATION = $\mu_{max,\,E.hux}$

CO_2fromDIC,alkalinity

= CO_2 calculated from DIC and alkalinity based on the CO2SYSTM program by Lewis and Wallace (http://cdiac.esd.ornl.gov/ oceans/co2rprt.html), using K_1 and K_2 according to *Roy et al.* [1993], and other dissociation constants as compiled by *Millero* [1995].

DIFx = $k_{dif} \times (x_{dld} - x_{mld})$

POTFLUX

= DICfromAlkalinity$_{potflux}CO_{2,air}$ - DIC$_{potflux}$. Alkalinity$_{potflux}$ and DIC$_{potflux}$ are calculated after mineralization of all particulate and organic carbon in the mixed layer. DICfromAlkalinity$_{potflux}CO_{2,air}$ works like CO_2fromDIC,alkalinity.

SEDIMENTATION

= $V_{sink} \times 3600 \times 24$ / mld. The sinking speed (V_{sink}) is calculated from Stokes' law by interpolation of the following equations:

V_{sink} = $(2 \times V \times g \times \Delta\rho / (A \times \rho \times C_d)^{0.5}$

Re = $V_{sink} \times \rho \times /\eta$

C_d = intercept × Re^{power}

The relationship between the drag coefficient (C_d) and the Reynolds number (Re) was of the form derived by *Aldredge and Gotschalk* [1988] and the parameter values are between those for diatom-dominated marine snow ($C_d = 105 \times Re^{-0.97}$) and other marine snow ($C_d = 95 \times Re^{-1.87}$, [*Alldredge and Gotschalk*, 1988]). In the model, intercept = 100. In the sensitivity analysis the value of power is varied to obtain sedimentation rates that were comparable to those obtained by using fixed rates of sedimentation between 0.02 and 0.12 d^{-1} [*van der Wal et al.*, 1995]. V, A and r are the volume, area and radius of the fecal pellets that constituted the main part of the sedimented material during the North Sea bloom (see *van der Wal et al.* [1995] for details on the collection of samples). Here $V = 3 \times 10^{-13}$ m^3, $A = 2.14 \times 10^{-9}$ m^2, $r = 4.153 \times 10^{-5}$ m, ρ is the density of seawater= 1.0267 kg L^{-1}, g is the gravitational acceleration = 9.8 m s^{-2}, and η is the kinematic viscosity = 1 g m^{-1} s^{-1}. The excess density of the sedimented material ($\Delta\rho = (M_{E\,hux} \times [POC_{E\,hux}] + 100 \times [CaCO_3]) / (M_{E\,hux} \times [POC_{E\,hux}] / \rho_{org} + 100 \times [CaCO_3] / \rho_{CaCO3} - \rho)$ was calculated from the effective densities of $CaCO_3$ and $POC_{E\,hux}$ in the ratio of their standing stocks. $M_{E\,hux}$ was estimated as 240 g mol^{-1}, since carbon is ~ 5% of wet biomass. Here ρ_{org} was estimated as 1.027 kg L^{-1}, while ρ_{CaCO3} = 1.66 kg L^{-1} was estimated from the density of calcite (2.8 kg L^{-1}) and the amount of water included in the coccosphere, which was estimated from the cell radius with and without coccosphere [*van Bleijswijk et al.*, 1994b] and the amount of $CaCO_3$ per coccosphere [*van Bleijswijk et al.*, 1991]. There was no sedimentation of $CaCO_3$ when $POC_{E\,hux}$ became 0 μM.

Acknowledgments. We would like to thank all the people who were involved in the field cruise and mesocosm experiments that were the basis for the presented model, with special thanks to Judith van Bleijswijk, Rob Kempers, Marcel Veldhuis, and Jorun Egge. We would like to thank Judith van Bleijswijk, Wil Buitenhuis, and the three reviewers for their helpful comments on the manuscript.

References

Alldredge, A.L., and C. Gotschalk, In situ settling behavior of marine snow, *Limnol. Oceanogr., 33*, 339-351, 1988.

Bakker, D.C.E, H.J.W de Baar, and U.V. Bathmann, Changes of carbon dioxide in surface waters during spring in the Southern Ocean, *Deep Sea Res., Part II, 44*, 91-128, 1997.

Broecker, W.S., Geochemical tracers and ocean circulation, *Evolution of physical oceanography*, edited by B.A. Warren and C. Wunsch, pp. 434-460, MIT Press, Cambridge, Mass., 1981.

Buitenhuis, E., J. van Bleijswijk, D. Bakker, and M. Veldhuis, Trends in inorganic and organic carbon in a bloom of *Emiliania huxleyi* in the North Sea, *Mar. Ecol. Prog. Ser., 143*, 271-282, 1996.

Buitenhuis, E.T., H.J.W. de Baar, and M.J.W. Veldhuis, Photosynthesis and calcification by *Emiliania huxleyi* (Prymnesiophyceae) as a function of inorganic carbon species, *J. Phycol., 35*, 949-959, 1999.

Chipman, D.W., J. Marra, and T. Takahashi, Primary production at 47°N and 20°W in the North Atlantic Ocean: a comparison between the ^{14}C incubation method and the mixed layer carbon budget, *Deep Sea Res., Part II, 40*, 151-169, 1993.

Crawford, D.W., and D.A. Purdie, Increase of PCO_2 during blooms of *Emiliania huxleyi*: Theoretical considerations on the asymmetry between acquisition of HCO_3^- and respiration of free CO_2, *Limnol. Oceanogr., 42*, 365-372, 1997.

Dong, L.F., N.A. Nimer, E. Okus, and M.J. Merrett, Dissolved inorganic carbon utilization in relation to calcite production in *Emiliania huxleyi* (Lohmann) Kamptner, *New Phytol., 123*, 679-684, 1993.

Goldman, J. C., and M. R. Dennett, Growth of marine bacteria in batch and continuous culture under carbon and nitrogen limitation. *Limnol. Oceanogr. 45*, 789-800, 2000.

Harris, R.P., Zooplankton grazing on the coccolithophore *Emiliania huxleyi* and its role in inorganic carbon flux, *Mar. Biol., 119*, 431-439, 1994.

Jasper, J.P., J.M. Hayes, A.C. Mix, and F.G. Prahl, Photosynthetic fractionation of ^{13}C and concentrations of dissolved CO_2 in the central equatorial Pacific during the last 255,000 years, *Paleoceanography, 9*, 781-798, 1994.

Koshikawa, H., S. Harada, M. Watanabe, K. Kogure, T. Ioriya, K. Kohata, T. Kimura, K. Sato, and T. Akehata, Influence of plankton community structure on the contribution of bacterial production to metazooplankton in a coastal mesocosm, *Mar. Ecol. Prog. Ser., 186*, 31-42, 1999.

Michaelis, M., and M.L. Menten, Kinetics of invertase action, *Zeitschrift Biochemie, 49*, 333, 1913.

Millero, F.J, Thermodynamics of the carbon dioxide system in the oceans, *Geochim. Cosmochim. Acta, 59*, 661-677, 1995.

Milliman, J. D., P. J. Troy, W. M. Balch, A. K. Adams, Y.-H. Li, and F. T. Mackenzie, Biologically mediated dissolution of calcium carbonate above the chemical lysocline? *Deep Sea Res., Part I*, 46, 1653-1669, 1999.

Paasche, E., Roles of nitrogen and phosphorus in coccolith formation in *Emiliania huxleyi* (Prymnesiophyceae), *Eur. J. Phycol., 33*, 324-330, 1998.

Ploug, H., H.-P. Grossart, F. Azam, and B. B. Jørgenson, Photosynthesis, respiration, and carbon turnover in sinking marine snow from surface waters of Southern California Bight: implications for the carbon cycle in the ocean, *Mar. Ecol. Prog. Ser., 179*, 1-11, 1999.

Redfield, A.C., B.H. Ketchum, and F.A. Richards, The influence of organisms on the composition of sea-water, *The Sea*, vol. 2, edited by M.N. Hill, pp. 26-77, Wiley-Interscience, New York, 1963.

Robertson, J.E., C. Robinson, D.R. Turner, P. Holligan, A.J. Watson, P. Boyd, E. Fernandez, and M. Finch, The impact of a coccolithophore bloom on oceanic carbon uptake in the northeast Atlantic during summer 1991, *Deep Sea Res. I, 41*, 297-314, 1994.

Roy, R.N., L.N. Roy, K.M. Vogel, C. Porter-Moore, T. Pearson, C.E. Good, F.J. Millero, and D.M. Campbell, The dissociation constants of carbonic acid in seawater at salinities 5 to 45 and temperatures 0 to 45°C, *Mar. Chem., 44*, 249-267, 1993.

Stolte, W., Size-dependent restrictions on competition for nutrients by marine phytoplankton, Ph.D. thesis, 122 pp., Rijksuniversiteit Groningen, Groningen, The Netherlands, 1996.

Taylor, A.H., A.J. Watson, M. Ainsworth, J.E. Robertson, and D.R. Turner, A modelling investigation of the role of phytoplankton in the balance of carbon at the surface of the North Atlantic, *Glob. Biogeochem. Cycles, 5*, 151-171, 1991.

Ulrich-Rich, J., D.A. Hansell, and M.R. Roman, Analysis of copepod

fecal pellet carbon using a high temperature combustion method. *Mar. Ecol. Prog. Ser., 171*, 199-208, 1998.

Urban, J.L., D. Deibel, and P. Schwinghamer, Seasonal variation in the densities of fecal pellets produced by *Oikopleura vanhoeffeni* (C. Larvacea) and *Calanus finmarchicus* (C. Copepoda), *Mar. Biol., 117*, 607-613, 1993.

Van Bleijswijk, J.D.L., and M.J.W. Veldhuis, In situ gross growth rates of *Emiliania huxleyi* in enclosures with different phosphate loadings revealed by diel changes in DNA content, *Mar. Ecol. Prog. Ser., 121*, 271-277, 1995.

Van Bleijswijk, J., P. van der Wal, R. Kempers, and M. Veldhuis, Distribution of two types of *Emiliania huxleyi* (Prymnesiophyceae) in the northeast atlantic region as determined by immunofluorescence and coccolith morphology, *J. Phycol., 27*, 566-570, 1991.

Van Bleijswijk, J.D.L., E.S. Kempers, P. van der Wal, P. Westbroek, J.K. Egge, and T. Lukk, Standing stocks of PIC, POC, PON and *Emiliania huxleyi* coccospheres and liths in seawater enclosures with different phosphate loadings, *Sarsia, 79*, 307-317, 1994a.

Van Bleijswijk, J.D.L., R.S. Kempers, and M.J. Veldhuis, Cell and growth characteristics of types A and B of *Emiliania huxleyi* (Prymnesiophyceae) as determined by flow cytometry and chemical analyses, *J. Phycol., 30*, 230-241, 1994b.

Van der Wal, P., J.D.L. van Bleijswijk, and J.K. Egge, Primary productivity and calcification rate in blooms of the coccolithophorid *Emiliania huxleyi* (Lohmann) Hay et Mohler developing in mesocosms, *Sarsia, 79*, 401-408, 1994.

Van der Wal, P., R.S. Kempers, and M.J.W. Veldhuis, Production and downward flux of organic matter and calcite in a North Sea bloom of the coccolithophore *Emiliania huxleyi*, *Mar. Ecol. Prog. Ser., 126*, 247-265, 1995.

Wanninkhof, R., Relationship between wind speed and gas exchange over the ocean, *J. Geophys. Res., 97*, 7373-7382, 1992.

Weiss, R.F., Carbon dioxide in water and seawater: the solubility of a non-ideal gas, *Mar. Chem., 2*, 203-215, 1974.

Wiebinga, C.J., Process studies of dissolved organic carbon and bacterioplankton in the ocean, Ph.D. thesis, 176 pp., Rijksuniversiteit Groningen, Groningen, Netherlands, 1999.

E. T. Buitenhuis, H. J. W. de Baar, and Paul van der Wal, Netherlands Institute for Sea Research, P.O. box 59, 1790 AB Texel, The Netherlands. (martinburo@email.com; debaar@nioz.nl; -)

(Received April 27, 2000; revised October 10, 2000; accepted October 31, 2000.)